FIRST-ORDER SPECKLE STATISTICS OF ULTRASOUND BREAST IMAGES SYNTHESIZED FROM A COMPUTATIONAL ANATOMY MODEL

Yi-Ting Shen[1,3] and James C. Lacefield[1,2,3]
Depts. of [1]Electrical & Computer Engineering and [2]Medical Biophysics, University of Western Ontario,
279 Thompson Engineering Building, London, Ontario, Canada N6A 5B9
[3]Imaging Research Laboratories, Robarts Research Institute, 100 Perth Drive, London, Ontario, Canada N6A 5K8
jlacefield@eng.uwo.ca

1. INTRODUCTION

Focus aberration produced by heterogeneous tissues can significantly reduce the spatial and contrast resolution of ultrasound imaging systems. Aberration can be particularly severe in breast imaging, which has limited the role of ultrasound in breast cancer diagnosis. Techniques based on adaptive inverse filtering[1,2] are now the state of the art in ultrasound aberration correction. Compared to thin phase screen methods, inverse filtering techniques are less dependent on assumptions about the spatial organization of aberrating structures in tissue, but realistic aberration models are still needed to evaluate new focusing methods and guide improvement of their performance.

This paper introduces a three-dimensional breast anatomy model and image synthesis method designed for future use in numerical studies of aberration correction and lesion detection in ultrasound imaging. First-order speckle statistics of synthetic B-mode ultrasound images are analyzed as an initial step toward validation of the model. The objective of this analysis is to demonstrate that the synthetic images possess the non-Rayleigh speckle statistics that are characteristic of clinical ultrasound breast images.[3]

2. METHODS

2.1 Breast anatomy model

A three-dimensional breast anatomy model was implemented using polyhedrons, spline curves, and fractal structures to represent skin, fat lobules, connective tissue, and lactiferous ducts in a manner similar to recently developed models for x-ray mammography simulation.[4,5] An unlimited number of realizations of breast anatomy are possible via random variation of user-specified structural parameters.

2.2 Ultrasound image synthesis

A two-dimensional cross-section with 0.015 mm sample spacing was extracted from the anatomy model and input to a *k*-space (spatial frequency domain) ultrasound propagation simulator.[6] Density, compressibility, and frequency-dependent attenuation parameters were assigned to each tissue type based on literature values, and compressibility variations with root-mean-square magnitude equal to 1% of the nominal values were added to produce randomly distributed scattering. B-mode imaging with a 192-element linear array was simulated using a synthetic aperture method. The simulated array had a 5 MHz centre frequency, a 3 MHz –6 dB bandwidth, and a one-wavelength element pitch. An image of a region without glandular tissue was synthesized with a 3.56×3.25 cm^2 field of view, six transmit focal zones, and dynamic receive focusing. A control image of a statistically homogeneous fat-mimicking phantom was also synthesized using the same procedure.

2.3 Image analysis

Each image was partitioned in sixteen 2.0×4.5 mm^2 regions of interest (ROI). The point signal-to-noise ratio (SNR), which is equal to the mean divided by the standard deviation of the echo signal magnitudes, was computed for each ROI. Wilcoxon signed-rank tests were performed to test null hypotheses that the point SNR of the fat-mimicking phantom and breast model images were equal to the theoretical value of 1.91 for Rayleigh-distributed speckle. *P*-values less than 0.05 were considered significant.

Empirical distribution function (EDF) tests using the Anderson-Darling A^2 statistic[7] were also performed to evaluate the goodness of fit of the Rayleigh probability density function (PDF) to histograms of echo magnitudes in the synthesized images. A^2 statistics for each ROI were compared to 1.321, which is the critical value at significance level $\alpha = 0.05$ for an EDF test of the Weibull distribution[7] (the Rayleigh PDF is a limiting case of the Weibull PDF). An A^2 statistic less than the critical value is considered evidence that the data were sampled from the hypothesized PDF.

3. RESULTS

The cross section through the breast anatomy model and the resultant synthetic B-mode image are shown in Fig. 1. Corresponding features are labelled in both panels.

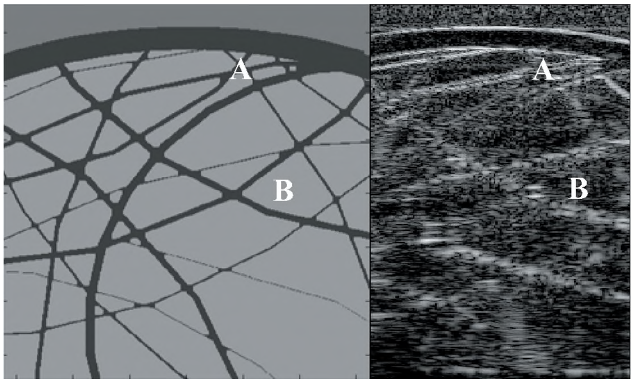

Fig. 1. Cross section from the breast anatomy model (left panel) and synthesized B-mode image (right panel) displayed using a 40-dB logarithmic grey scale. Dark pixels in the model represent skin and connective tissue, and lighter pixels in the interior of the model represent fat.

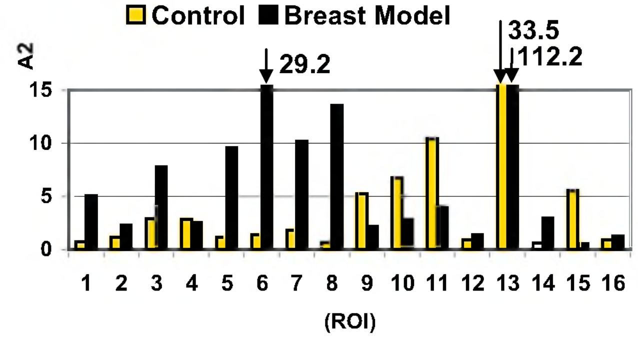

Fig. 2. A^2 goodness-of-fit statistics comparing the echo amplitude distribution in each ROI of the breast model and control images to the Rayleigh PDF. Speckle in an ROI is considered Rayleigh distributed at significance level 0.05 if A^2 is less than the critical value of 1.321.

The point SNR of the breast model image was 1.50 ± 0.30 (mean ± standard deviation over 16 ROI) and was significantly less than the theoretical value of 1.91 for Rayleigh-distributed speckle ($p < 0.001$). The point SNR in the control image of the fat-mimicking phantom was 1.89 ± 0.06, which was not significantly different from 1.91 ($p = 0.20$).

Figure 2 summarizes the A^2 statistics obtained for each ROI in the two images. In the breast model image, A^2 was less than the $\alpha = 0.05$ critical value of 1.321 in only two out of 16 ROI. For comparison, A^2 was less than the critical value in eight out of 16 ROI in the control image.

4. DISCUSSION

Fully developed Rayleigh speckle arises when a medium contains a large number of statistically homogeneous scatterers (*i.e.*, at least ten scatterers per resolution cell) that are randomly and uniformly positioned throughout the field of view, whereas a medium that violates one or more of these conditions produces non-Rayleigh speckle. The only scattering sites in the fat-mimicking phantom are random compressibility variations on the scale of the spatial sampling. The breast model also produces stronger scattering from the interfaces between the fat and the connective tissue septa, which should alter the speckle statistics of the resulting image.

The expected products of the simulations were a Rayleigh-distributed control image and a non-Rayleigh distributed image from the breast anatomy model, so the point SNR data are encouraging. The point SNR significantly less than 1.91 obtained in the breast model image is a characteristic of the speckle distributions observed in clinical ultrasound breast images.

The EDF test results provide further evidence that the breast model produced non-Rayleigh speckle. However, the observation that speckle in the control image was not consistently Rayleigh distributed indicates a need for further characterization of the image synthesis algorithm. The results may be improved by inclusion of additional realizations of both types of image. In addition, implementation of a goodness of fit test for the *K* distribution that describes clinical breast images[3] is desirable.

REFERENCES

[1]M. Tanter, J.-F. Aubry, J. Gerber, J.-L. Thomas, and M. Fink, J. Acoust. Soc. Am. **110**, 37-47 (2001).

[2]F. Lin and R. C. Waag, IEEE Trans. Ultrason. Ferroelectr. Freq. Contr. **49**, 739-755 (2002).

[3]R. C. Molthen, P. M. Shankar, J. M. Reid, F. Forsberg, E. J. Halpern, C. W. Piccoli, and B. B. Goldberg, Ultrasound Med. Biol. **24**, 93-100 (1998).

[4]P. R. Bakic, M. Albert, D. Brzakovic, and A. D. Maidment, Med. Phys. **29**, 2131-2139 (2002).

[5]K. Bliznakova, Z. Bliznakov, V. Bravou, Z. Kolitsi, and N. Pallikarakis, Phys. Med. Biol. **48**, 3699-3719 (2003).

[6]M. Tabei, T. D. Mast, and R. C. Waag, J. Acoust. Soc. Am. **111**, 53-63 (2002).

[7]R. B. D'Agostino and M. A. Stephens, *Goodness-of-Fit Techniques* (Marcel Dekker, Inc., New York, 1986), Chap. 4.

ACKNOWLEDGEMENTS

The authors thank Dr. Makoto Tabei, Dr. T. Douglas Mast, and Prof. Robert C. Waag for sharing the source code for the *k*-space propagation simulator. This research was supported by NSERC Discovery Grant 261323-03.